VI International Conference on Computational Bioengineering
ICCB 2015
M. Cerrolaza and S.Oller (Eds)

REAL-TIME MODELLING OF THE HEART USING THE PROPER ORTHOGONAL DECOMPOSITION WITH INTERPOLATION

R.R. RAMA[*,†], S. SKATULLA[*,†] AND C. SANSOUR[‡]

[*] Centre for Research in Computational and Applied Mechanics
University of Cape Town, South Africa
e-mail: rmxrit001@myuct.ac.za

[†]Computational Continuum Mechanics group, Civil Engineering Department
University of Cape Town, South Africa

[‡]Division of Material, Mechanics, and Structures
The University of Nottingham, United kingdom

Key words: Key Words: Reduced Order Method, Proper Orthogonal Decomposition with Interpolation, Moving Least Square Approximation, Heart Modelling, Cardiac Mechanics

Abstract. In this research, a reduced order method (ROM) called the Proper Orthogonal Decomposition with Interpolation (PODI) is used to drastically reduce computation time of highly complex and non-linear problems as encountered in simulating the heart. The idea behind the method is to first construct a database of pre-computed full-scale solutions using the Element Free Galerkin method (EFG), project the set of solutions to a low dimensional space, use the Moving Least Square method to carry out the interpolation for the problem at hand and project it back to the original high dimensional solution space. Calculations are carried out on a bi-ventricle model to investigate the performance and accuracy while varying one of the material parameters.

1 INTRODUCTION

In order to model the pumping heart, one needs to describe the non-linear elasticity and visco-elastic material behaviour of the heart muscle tissue [4, 11], the active contraction to eject the blood into the lungs and the systemic circulatory system[11], the electro-physiology pacing the contraction of the heart muscle[8] and the coupling of the blood circulatory system to the heart in terms of varying blood pressure and flow resistance[28]. However, in those mathematical models stated, complex non-linear partial and ordinary

differential equations are employed and need to be solved using iterative schemes. These computational calculations are extremely time consuming. In [23, 29, 15] and [30], it has been found that the required computational resources can vary from at least 16 to as much as 200 processors for calculation times ranging between 1 to 50 hours. For this reason, the application of such models has been very limited in the medical practise as they would be required to be run on common desktop or laptop machines. Hence, the solution proposed in this research is to use a Reduced Order Method (ROM) and amongst those, specifically, the so-called Proper Orthogonal Decomposition (POD).

The POD is a way of extracting information from a predefined set of data obtained from a set of experiments or simulated models using some statistical methods. It has the ability to capture important details or trends and represents them in terms of a set of numerical vectors known by several names such as *POD basis, Proper Orthogonal Modes (POM), empirical Eigenfunctions or empirical orthogonal functions*. The use of POD in solid mechanics is well established, e.g. [12, 1, 22, 12, 9], in particular analyzing the dynamics behaviour of structures.

One particular variant of POD this research will focus on is called the Proper Orthogonal Decomposition with interpolation method (PODI). It was developed by Ly and Tran [21], involves a collection of datasets of the structure under consideration describing its mechanics for a range of variations in terms of geometry, material properties, loading conditions etc. These datasets are used to interpolate the mechanics of a structure of the same category where its mechanical behaviour is unknown or has not been determined yet. In our case, the collection of datasets comprises of full-scale simulation results of the human heart obtained using the Element-Free Galerkin method(EFG) for different cardiac tissue parameters(such as stiffness, fibre orientation, ... etc). After the calculation, the results are then stored off-line in a database type format for ease of access. Recent research carried out by Niroomandi et al. and Coelho et al. have found that such approach allows for sub-second calculation times to be achieved and therefore making high frequency computation feasible [24, 3]. Regarding the interpolation technique used, the Moving Least Square approximation(MLS) has been chosen due to its ability in scaling up smoothly to several dimensions when multi-parametric simulations will be carried out while still generating accurate results[3].

The application of the POD method to heart modelling will be presented in this paper in the following structure. In Section 2.1, the ROM will be revisited with a particular reference to the POD method. The Proper Orthogonal Decomposition with Interpolation will then be elaborated in Section 2.2. In Section 3, the cardiac mechanics equations along with the model used for simulation of the heart will be introduced. Our methodology will subsequently be detailed in Section 4 before we finally present the results of our implementation in Section 5.

2 REDUCED ORDER METHOD

Reduced Order Method(ROM) is a technique commonly used to decrease the complexity of large system of equations. This is achieved by compressing the whole system to such a point that accuracy is not, in an excessive way, negatively impacted and that the general behaviour of the problem, e.g the mechanics, is preserved. One widely used method classified as a ROM is called the *Proper orthogonal decomposition* and will be utilised in this research in the form of *Proper orthogonal decomposition with interpolation* to achieve real-time modelling of the heart.

2.1 Proper Orthogonal Decomposition

The Proper Orthogonal Decomposition is a method that can be used to extract features from any dataset consisting of either linear or non-linear data. In the literature, it is usually found in the form of Kharhunen-Loève Decomposition (KLD) [20, 13], Singular Value Decomposition (SVD) or Principal Component Analysis (PCA). Even though each of them have different derivations, Wu et al. [31] showed the equivalence between those methods and how they can all produce the same solution.

In this paper, KLD has been chosen to explain the POD. Suppose $\mathbf{U}$ is an ensemble set of displacement fields, describing the state of deformation of a body at discrete time steps t_i , $i = 1 \dots n$, which have been defined over a one-dimensional spatial domain $0 \leq x \leq 1$.

$$\mathbf{U} = \left\{ \mathbf{u}^1, \mathbf{u}^2, \dots, \mathbf{u}^n \right\}, \tag{1}$$

where for the total number of time steps it holds $n << m$, and m is the number of displacement degrees of freedom. If the displacement field is approximated by a set of basis vectors, $\widetilde{\mathbf{\Phi}}$, and coefficients, $\boldsymbol{\alpha}$, through

$$\mathbf{u}^i = \sum_{j=1}^{n} \alpha_j^i \widetilde{\mathbf{\Phi}}_j, \tag{2}$$

then, the KLD problem is posed as an optimality scheme which requires one to maximise the average projection of $\mathbf{U}$ onto $\widetilde{\mathbf{\Phi}}$ while being subjected to the constraint of $\widetilde{\mathbf{\Phi}}$ being orthonormal:

$$\begin{aligned} \max_{\widetilde{\mathbf{\Phi}}} \quad & \left\langle \left| \left(\mathbf{U}, \widetilde{\mathbf{\Phi}} \right) \right|^2 \right\rangle \\ \text{s.t.} \quad & \|\widetilde{\mathbf{\Phi}}\|^2 = \mathbf{1}, \end{aligned} \tag{3}$$

with $(\mathbf{f}, \mathbf{g}) = \int_0^1 \mathbf{f}(x)\mathbf{g}^{\mathrm{T}}(x)dx$, $\langle \cdot \rangle$ being the averaging operation and $\|\mathbf{f}\| = (\mathbf{f}, \mathbf{f})^{\frac{1}{2}}$. After solving (3) with the help of the Lagrange multiplier method, the following eigenvalue problem was obtained:

$$\left(\mathbf{R}, \widetilde{\mathbf{\Phi}} \right) = \boldsymbol{\lambda} \widetilde{\mathbf{\Phi}} \qquad \text{with} \quad \mathbf{R} = \frac{1}{n} \mathbf{U}\mathbf{U}^{\mathrm{T}}. \tag{4}$$

Solving the above produces a set of eigenfunctions which is optimal to the optimisation problem stated in (3). $\mathbf{R}$ is usually referred to as the *kernel* and is a positive semi-definite symmetric matrix [26]. It is also alternatively defined as the *auto-correlation* matrix [6], whose eigenvalues (so-called *Proper Orthogonal Values*, POVs) and eigenfunctions (so-called *Proper Orthogonal Modes*, POMs) are represented by $\boldsymbol{\lambda}$ and $\widetilde{\boldsymbol{\Phi}}$ respectively.

If $\mathbf{R}$ is computed from a whole set of data $m \times n$, with m being very large, then the resulting matrix would be of size $m \times m$ and extremely large as well. This therefore leads to an increase in computational time to find $\boldsymbol{\lambda}$ and $\widetilde{\boldsymbol{\Phi}}$. One method, which is widely used to reduce the system, has been proposed by Sirovich and is commonly known as the *snapshot method* [25]. If the number of columns (i.e number of snapshots or time steps, n) is smaller than m, then (4) can be reduced from an m to an n size system of equations which will therefore decrease the size of the auto-correlation matrix to $n \times n$. To do so, (4) is reformulated as follows:

$$(\mathbf{C}, \boldsymbol{\xi}) = \boldsymbol{\lambda}\boldsymbol{\xi} \qquad \text{with} \;\; \mathbf{C} = \frac{1}{n}\mathbf{U}^{\mathrm{T}}\mathbf{U}. \tag{5}$$

The eigenvalues of $\mathbf{C}$ are the same as those obtained from (4) and can hence be defined to be the POVs. However, the associated eigenvectors are not the POMs. To recover the latter, the following equation is required [18]:

$$\widetilde{\boldsymbol{\Phi}}^{i} = \frac{1}{\sqrt{n\lambda_i}}\mathbf{U}\boldsymbol{\xi}^{i}. \tag{6}$$

The choice of POMs are very essential in minimising the loss in accuracy of a set of solutions. According to Kerschen et al., the POVs can be used as a guideline to do so [14]. In [2], Barbic and James showed that for each POM, there is a corresponding POV, which is represented by the eigenvalue obtained from the SVD or KLD method. Usually, the POM represents a modal mode which characterises, in a mechanical problem, a specific deformation of the domain while the corresponding POV is attributed to the captured energy from that particular deformation [14]. In order to find the total energy discarded when reducing the dataset, Falkiewicz and Cesnik produced the following equation in [7]:

$$\varepsilon_{\mathrm{rel}} = \frac{\sum_{f=1}^{n-r} \lambda_f}{\sum_{g=1}^{n} \lambda_g} \times 100, \tag{7}$$

with r being the number of POMs conserved and $r < n$. In that sense, in order to find a proper balance between selecting a few POMs and conserving the greatest amount of energy, the POD basis, associated with the highest POVs is selected as the former represents the dominant modes of deformation. Interestingly, it was found that with very few modes, one can easily conserve up to 99% of the energy in the system. In [19], Lin et al. noted that, with their set of data comprising of 24 snapshots, only the first two

POVs were enough to achieve an energy conservation of 99.9997%, leading us to believe that a 99 % energy threshold is enough to achieve a reasonable accuracy.

2.2 Proper Orthogonal Decomposition with Interpolation

For the purpose of real-time modelling, the direct application of POD to system of equations is not suitable. When applied to the finite element method (FEM), only the solving part of the overall process is accelerated while the preprocessing time and repetitive equation system assembly time prohibit a drastic drop in calculation time. Hence, in order to circumvent this problem, the *Proper Orthogonal Decomposition with Interpolation* (PODI), developed by Ly and Tran [21], has been employed in this work. Their idea starts by first constructing the matrix $\mathbf{U}$ from an ensemble of displacement vector, $\{\mathbf{u}^1, \ldots, \mathbf{u}^p\}$. Each dataset, $\mathbf{u}^a$, where $\mathbf{u}^a \in \{\mathbf{u}^1, \ldots, \mathbf{u}^p\}$, corresponds to a set of parameter, $\boldsymbol{\theta}^a$, where $\boldsymbol{\theta}^a \in \{\boldsymbol{\theta}^1, \ldots, \boldsymbol{\theta}^p\}$. Here, $\{\boldsymbol{\theta}^1, \ldots, \boldsymbol{\theta}^p\}$ is defined as a sequence of parameter sets.

From there, the POD calculation is carried out and used to transfer the datasets to a low dimensional space using the POMs, where an interpolation technique is set up to find the adequate solution. Once this is done, the solution is then projected back to the high-dimensional space. The derivation of the method is given by first expressing $\mathbf{U}$ in matrix notation:

$$\mathbf{U} \approx \boldsymbol{\Phi}\boldsymbol{\Psi} \tag{8}$$

and then expanding (8) in matrix form:

$$\begin{bmatrix} u_1^1 & u_1^2 & \cdots & u_1^{p-1} & u_1^p \\ u_2^1 & u_2^2 & & & u_2^p \\ \vdots & & \ddots & & \vdots \\ u_{m-1}^1 & & & \ddots & u_{m-1}^p \\ u_m^1 & u_m^2 & \cdots & u_m^{p-1} & u_m^p \end{bmatrix} \approx \begin{bmatrix} \phi_1^1 & \phi_1^2 & \cdots & \phi_1^r \\ \phi_2^1 & \phi_2^2 & \cdots & \phi_2^r \\ \vdots & \vdots & \cdots & \vdots \\ \phi_{m-1}^1 & \phi_{m-1}^2 & \ddots & \phi_{m-1}^r \\ \phi_m^1 & \phi_m^2 & \cdots & \phi_m^r \end{bmatrix} \begin{bmatrix} \psi_1^1 & \psi_1^2 & \cdots & \psi_1^p \\ \psi_2^1 & \psi_2^2 & \cdots & \psi_2^p \\ \vdots & \vdots & \cdots & \vdots \\ \psi_{r-1}^1 & \psi_{r-1}^2 & \ddots & \psi_{r-1}^p \\ \psi_r^1 & \psi_r^2 & \cdots & \psi_r^p \end{bmatrix}, \tag{9}$$

where a single displacement vector, $\mathbf{u}^a$, can be defined as:

$$\mathbf{u}^a \approx \psi_1^a \boldsymbol{\Phi}^1 + \psi_2^a \boldsymbol{\Phi}^2 + \cdots + \psi_r^a \boldsymbol{\Phi}^r. \tag{10}$$

Now, let's suppose that an unknown displacement field, $\hat{\mathbf{u}}$ (with $\hat{\mathbf{u}} \notin \{\mathbf{u}^1, \ldots, \mathbf{u}^p\}$), which corresponds to the set of parameters $\hat{\boldsymbol{\theta}}$ $\left(\text{where } \boldsymbol{\theta}^1 < \hat{\boldsymbol{\theta}} \leq \boldsymbol{\theta}^p \text{ and } \hat{\boldsymbol{\theta}} \notin \{\boldsymbol{\theta}^1, \ldots, \boldsymbol{\theta}^p\}\right)$, is to be found using the above POD basis. Therefore, (10) can be re-written as

$$\hat{\mathbf{u}} \approx \hat{\psi}_1 \boldsymbol{\Phi}^1 + \hat{\psi}_2 \boldsymbol{\Phi}^2 + \cdots + \hat{\psi}_r \boldsymbol{\Phi}^r. \tag{11}$$

In (11), $\hat{\mathbf{u}}$ cannot be found as $\hat{\boldsymbol{\Psi}} = \left(\hat{\psi}_1, \hat{\psi}_2, \ldots, \hat{\psi}_r, \right)$ is unknown and $\hat{\boldsymbol{\Psi}} \notin \{\boldsymbol{\Psi}^1, \ldots, \boldsymbol{\Psi}^p\}$. In this case, Ly and Tran [21] suggested to interpolate $\hat{\boldsymbol{\Psi}}$ from matrix $\boldsymbol{\Psi}$ through:

$$\hat{\mathbf{\Psi}} = \mathbf{\Psi}\mathbf{N}, \tag{12}$$

where $\mathbf{N}$ are the interpolants that can be derived from

$$\hat{\boldsymbol{\theta}} = \mathbf{\Theta}\mathbf{N}, \tag{13}$$

as $\hat{\boldsymbol{\theta}}$ and $\mathbf{\Theta}$ are both known. $\mathbf{\Theta} = (\boldsymbol{\theta}^1, \boldsymbol{\theta}^2, \ldots, \boldsymbol{\theta}^p)$ and is a matrix. Each row of that matrix is defined by a specific parameters of a particular set of parameters while the columns are the different set of parameters. In this research, the Moving Least Square Approximation method (MLS)[16] was chosen as it can deal with problems of arbitrary dimensionality and different size of data points.

3 CARDIAC MECHANICS AND MODEL

In this paper, we intend to model a bi-ventricle model(BV) which contains the left and right cavity only. The heart stage that will be looked at corresponds to the diastolic filling of the ventricular cavities with blood. To have a close-to-real heart muscle tissue behaviour, the material of our BV has been defined by an exponential function coupled with an incompressibility term. The non-linear orthotropic hyperelastic strain energy function used in this research is based on Legner et al. [17]:

$$W = \frac{A}{2}\left(e^{Q} - 1\right) + A_{\text{compr}}\left[\mathrm{J}\ln\left(\mathrm{J}\right) - \mathrm{J} + 1\right], \tag{14}$$

where J denotes the Jacobian and the exponent

$$\begin{aligned} Q =& a_1\left(\mathrm{tr}\left(\mathbf{M}_1\mathbf{E}\right)\right)^2 + a_2\left(\mathrm{tr}\left(\mathbf{M}_2\mathbf{E}\right)\right)^2 + a_3\left(\mathrm{tr}\left(\mathbf{M}_3\mathbf{E}\right)\right)^2 + \\ & a_4\left(\mathrm{tr}\left(\mathbf{M}_1\mathbf{E}\right)^2\right) + a_5\left(\mathrm{tr}\left(\mathbf{2}_5\mathbf{E}\right)^2\right) + a_6\left(\mathrm{tr}\left(\mathbf{M}_3\mathbf{E}\right)^2\right) \end{aligned} \tag{15}$$

is formulated in terms of the Green strain tensor

$$\begin{aligned} \mathbf{E} =& \hat{E}_{11}\mathbf{V}_1\otimes\mathbf{V}_1 + \hat{E}_{22}\mathbf{V}_2\otimes\mathbf{V}_2 + \hat{E}_{33}\mathbf{V}_3\otimes\mathbf{V}_3 + \hat{E}_{12}\left(\mathbf{V}_1\otimes\mathbf{V}_2 + \mathbf{V}_2\otimes\mathbf{V}_1\right) + \\ & \hat{E}_{13}\left(\mathbf{V}_1\otimes\mathbf{V}_3 + \mathbf{V}_3\otimes\mathbf{V}_1\right) + \hat{E}_{23}\left(\mathbf{V}_2\otimes\mathbf{V}_3 + \mathbf{V}_3\otimes\mathbf{V}_2\right) \end{aligned} \tag{16}$$

associated material constants $a_i, i = 1\ldots6$ and a set of structural tensors

$$\mathbf{M}_1 = \mathbf{V}_1\otimes\mathbf{V}_1, \qquad \mathbf{M}_2 = \mathbf{V}_2\otimes\mathbf{V}_2, \qquad \mathbf{M}_3 = \mathbf{V}_3\otimes\mathbf{V}_3. \tag{17}$$

The structural tensors refer to the preferred material directions of myocardial tissue, i.e. fibre axis, $\mathbf{V}_1$, $\mathbf{V}_2$ and $\mathbf{V}_3$. The remaining constants are the stress-scaling factor A and the A_comp, the latter controlling the compressibility of the material. The coefficients a_i have been converted from [27] and are given in table 1.

Parameter	Coefficient
a_1	-6
a_2	-5
a_3	9
a_4	12
a_5	12
a_6	-6

Table 1: Coefficients of a_i

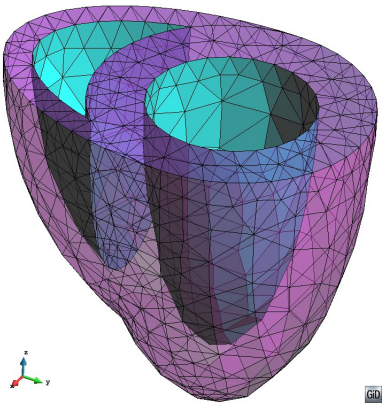

Figure 1: Fibre direction of a bi-ventricular model

Fig.1 introduces the bi-ventricle model (BV) that will be used for simulations. The geometry has been adapted from [10] where two ellipsoids were trimmed and fused together to obtain a visually realistic heart model.

The geometrical model was discretised by 823 nodes, hence resulting in a system of equation with 2469 degrees of freedom (DOFs). The boundary conditions applied were as follows: The left ventricle cavity was subjected to a uniform pressure of 1 kPa over the endocardial wall, while the right ventricular one was lowered to 0.2 kPa[10]. Due to the non-linearity of the problem in terms of strain and stress, the problem was solved incrementally by applying the cavity pressures in 100 steps. The displacement boundary conditions used by Legner et al. [17] were applied to both ventricles, that is, the base of the heart is not allowed to move along the heart's longitudinal axis while the cavity wall, at the base, is fixed in all 3 coordinate directions.

4 METHODOLOGY

In this section, a step-by-step description of our approach to setup the PODI algorithm is given. The layout of our implementation has been split into 3 main processes: Database construction, reduced order calculation and finally, post-processing. Each process is discussed below.

- **Database construction:** The first step of the database construction procedure was to create each dataset. The latter consisted of solution fields, such as displacement, stress and strain, that has been stored off-line for each time-step of a simulation. An in-house code called SESKA, which is based on the Element Free Galerking method(EFG)[5] was run on a desktop computer equipped with an Intel i7 processor (4 physical cores clocked at 3.4 GHz) and 8 GB of memory in order to produce these datasets.
  Regarding the database itself, a very basic database management system was used where all dataset was stored locally on a hard-drive, structured into folders. The entry

of each dataset was then registered in a comma-separated values (CSV) file, which can be generated by an editor program or a spreadsheet software. The latter will only be used to store parameter values(such as A and A_{comp}) along with the location of the dataset on the drive.

- **ROM Calculation:** Before starting the actual calculation, the matrix U needs to be assembled. This is done by firstly feeding the set of parameters of the problem at hand, into a selection algorithm which will query the database and pick the datasets which feature the closest match in terms of problem defining parameters. These datasets are the "neighbouring nodes" in the MLS-based PODI calculation. Once isolated, the chosen dataset are then used to assemble different $\mathbf{U}$ matrices. At the end, each U matrix will be setup for a particular result type and a specific time-step.
  After selecting the dominant modes of a particular $\mathbf{U}$ matrix, the latter is then reduced using $\mathbf{\Phi}^{-1}\mathbf{U} \approx \mathbf{\Psi}$ from (8). For the interpolation process in the PODI method, the Moving Least approximation scheme is then executed to compute the interpolants which will calculate the coefficients. In order to recover the full degrees of freedom solution from the coefficient, (11) is then used.

- **Postprocessing and Validation:** Once the PODI calculation is completed, the results will be saved and viewed by a post-processing software called GiD (CIMNE International Center for Numerical Methods in Engineering). For the validation process, the error in the PODI calculation is then compared with the solution computed using EFG, which is assumed to be the exact solution. The error calculation is given as the ℓ_2 error norm:

$$\varepsilon_{\ell_2} = \frac{\left\|\mathbf{U}^{\mathrm{PODI}} - \mathbf{U}^{\mathrm{EFG}}\right\|}{\left\|\mathbf{U}^{\mathrm{EFG}}\right\|} \times 100 \tag{18}$$

5 NUMERICAL EXAMPLES

A small BV model database of A ranging from 0.30 to 0.40 at an interval of 0.01 was constructed. The total number of datasets that was available for the calculation was 10 only, as shown in Table 2. $A = 0.35$ was not included in the databased as it was considered to be the unknown parameter for which the PODI simulation will be carried out.

Dataset ID	1	2	3	4	5	6	7	8	9	10
A	0.30	0.31	0.32	0.33	0.34	0.36	0.37	0.38	0.39	0.40

Table 2: Biventricle Model database with varying A values

The PODI calculation was completed in 0.94 s, compared to the EFG simulation which took about 20 h using 2 physical cores. The displacement field PODI calculation took only

0.15 s (6.67 GHz). This computation time includes the arrangement of the data matrix **U**, as stated in section 4, the SVD calculation using the LAPACK Fortran-library, the selection of the most dominant POMs, the reduction of the data matrix, the interpolation of the results, and the projection of the result back to the high dimensional space for all the 100 calculation steps. The number of dataset mobilised in the MLS influence domain was 6: 0.32, 0.33, 0.34, 0.36, 0.37 and 0.38 respectively. The energy level conservation was set to a minimum of 99 %. However when the SVD decomposition was carried out, the most dominant mode already accounted for 99.98 %. Hence, only one POM was found to be enough to represent the whole behaviour of the heart per calculation step, reducing the matrix size from 2469×6 to 1×6.

Regarding the error between the exact and interpolated results, the ℓ_2 error norm was computed for the displacement field and found to be only 1.1×10^{-3}. The PODI computations for stress and strain results lead to an average energy conservation of 99.97%, where only 1 POM was required to surpass the minimum target energy conservation. Compared to the displacement results, the error was similarly small as the ℓ_2 error norm of the stress and strain result was only 1.49×10^{-3} and 1.54×10^{-3} respectively.

Another result that is usually considered important in cardiac mechanics modelling, is the relationship between the cavity volumes of the ventricles and the cavity pressure. In this case, we also compared the approximated and the reference solution curve of that relationship. The overall deformation behaviour of the cavity was found to be here also almost the same as the error was only 5.11×10^{-6}.

6 CONCLUSIONS

The results obtained from this research show that real-time modelling of the heart can be carried out successfully on a normal desktop machine. Even though a loss of accuracy was noted, it could be largely acceptable, in particular considering the dramatic speed-up in computation time. This, therefore, makes the PODI method very attractive as the mechanics behaviour of the heart is still fully preserved. Following those encouraging results, the next step of this research is to extend the PODI method to interpolate datasets of hearts with different geometries and mesh discretisations. The latter is important because the structural composition of real heart varies between individuals.

7 ACKNOWLEDGEMENT

This research has been supported by the Centre for High Performance Computing South Africa and the National Research Foundation of South Africa (Grant Number 90528).

References

[1] M. Amabili, A. Sarkar, and M. Padoussis. Chaotic vibrations of circular cylindrical shells: Galerkin versus reduced-order models via the proper orthogonal decompo-

sition method. *Journal of Sound and Vibration*, 290(35):736 – 762, March 2006. doi:10.1016/j.jsv.2005.04.034.

[2] J. Barbic and D. James. Real-time subspace integration for st.venant-kirchhoff deformable models. *ACM Transactions on Graphics (TOG) - Proceedings of ACM SIGGRAPH 2005*, 24(3):982–990, July 2005. doi:10.1145/1073204.1073300.

[3] R. F. Coelho, P. Breitkopf, C. Knopf-Lenoir, and P. Villon. Bi-level model reduction for coupled problems. application to a 3d wing. *Structural and Multidisciplinary Optimization*, 39(4):401–418, October 2009. doi:10.1007/s00158-008-0335-3.

[4] L. L. Demer and F. C. P. Yin. Passive biaxial mechanical properties of isolated canine myocardium. *Journal of Physiology*, 339:615–630, 1983.

[5] J. Dolbow and T. Belytschko. An introduction to programming the meshless element f reegalerkin method. *Archives of Computational Methods in Engineering*, 5(3):207–241, September 1998. doi:10.1007/BF02897874.

[6] P. Druault, P. Guibert, and F. Alizon. Use of proper orthogonal decomposition for time interpolation from piv data: Application to the cycle-to-cycle variation analysis of in-cylinder engine flows. *Experiments in Fluids*, 39:1009–1023, 2005. doi:10.1007/s00348-005-0035-3.

[7] N. J. Falkiewicz and C. E. S. Cesnik. Proper orthogonal decomposition for reduced-order thermal solution in hypersonic aerothermielastic simulation. *AIAA Journal*, 49 (5):994–1009, May 2011. doi:10.2514/1.J050701.

[8] P. C. Franzone and L. Guerri. Spreading of excitation in 3-d models of the anisotropic cardiac tissue. i. validation of the eikonal model. *Mathematical Biosciences*, 113(2): 145–209, February 1993. doi:10.1016/0025-5564(93)90001-Q.

[9] I. T. Georgiou and J. Sansour. Analyzing the finite element dynamics of nonlinear in-plane rods by the method of proper orthogonal decomposition. In S. Idelsohn, E. Onate, and E. Dvorkin, editors, *Computational Mechanics, New Trends and Applications*, Barcelona, Spain, 1998. CIMNE.

[10] S. Göktepe, S. Acharya, J. Wong, and E. Kuhl. Computational modelling of passive myocardium. *International Journal for Numerical Methods in Biomedical Engineering*, 27:1–12, 2011. doi:10.1002/cnm.1402.

[11] J. Guccione, L. Waldman, and A. McCulloch. Mechanics of active contraction in cardiac muscle: part iicylindricalmodels of the systolic left ventricle. *Journal of Biomechanical Engineering*, 115(1):82–90, February 1993. doi:10.1115/1.2895474.

[12] S. Han and B. Feeny. Application of proper orthogonal decomposition to structural vibration analysis. *Mechanical Systems and Signal Processing*, 17(5):989 – 1001, September 2003. doi:10.1006/mssp.2002.1570.

[13] K. Karhunen. Zur spektraltheorie stochastischer prozesse. *Ann. Acad. Sci. Fennicae*, A1:34, 1946.

[14] G. Kerschen, J.-C. Golinval, A. Vakakis, and L. Bergman. The method of proper orthogonal decomposition for dynamical characterisation and order reduction of mechanical systems: An overview. *Nonlinear Dynamics*, 41(1-3):147–169, August 2005. doi:10.1007/s11071-005-2803-2.

[15] P. Lafortune, R. Ars, M. Vzquez, and G. Houzeaux. Coupled electromechanical model of the heart: Parallel finite element formulation. *International Journal for Numerical Methods in Biomedical Engineering*, 28:72–86, 2012. doi:10.1002/cnm.1494.

[16] P. Lancaster and K. Salkauskas. Surfaces generated by moving least squares methods. *Mathematics of Computation*, 37:141–158, 1981. doi:10.1090/S0025-5718-1981-0616367-1.

[17] D. Legner, S. Skatulla, J. MBewu, R. R. Rama, B. D. Reddy, C. Sansour, N. H. Davies, and T. Franz. Studying the influence of hydrogel injections into the infarcted left ventricle using the element-free galerkin method. *International Journal for Numerical Methods in Biomedical Engineering*, 30:416429, 2014. doi:10.1002/cnm.2610.

[18] H. Li, Z. Luo, and J. Chen. Numerical simulation based on pod for two-dimensional solute transport problems. *Applied Mathematical Modelling*, 35(5):2489–2498, May 2011. doi:10.1016/j.apm.2010.11.064.

[19] W. Z. Lin, Y. J. Zhang, and E. P. Li. Proper orthogonal decomposition in the generation of reduced order models for interconnects. *IEEE Transactions on Advanced Packaging*, 31(3):627, August 2008. doi:10.1109/TADVP.2008.927820.

[20] M. Loève. Function aleatoire de second ordre. *Comptes Rendus Acad. Sci. Paris*, -: 220, 1945.

[21] H. V. Ly and H. T. Tran. Modeling and control of physical processes using proper orthogonal decomposition. In H. Banks, K. Bowers, and J. Lund, editors, *Computation and control VI proceedings of the sixth Bozeman conference*, volume 33, pages 223 – 236. Mathematical and Computer Modelling, January and February 2001. doi:10.1016/S0895-7177(00)00240-5.

[22] R. Mariani and D. Dessi. Analysis of the global bending modes of a floating structure using the proper orthogonal decomposition. *Journal of Fluids and Structures*, 28(0): 115134, January 2012. doi:10.1016/j.jfluidstructs.2011.11.009.

[23] S. A. Niederer and N. P. Smith. The role of the frankstarling law in the transduction of cellular work to whole organ pump function: A computational modeling analysis. *PLoS Computational Biology*, 5(4):1–18, April 2009. doi:10.1371/journal.pcbi.1000371.

[24] S. Niroomandi, I. Alfaro, E. Cueto, and F. Chinesta. Real-time deformable model of non-linear tissues by model reduction techniques. *Computer Methods and Programs in Biomedicine*, 91:223–231, 2008. doi:10.1016/j.cmpb.2008.04.008.

[25] L. Sirovich. Turbulence and the dynamics of coherent structures. *Applied Mathematics*, XLV(3):561–82, 1987.

[26] B.-T. Tan, K. Willcox, and M. Damodaran. Applications of proper orthogonal decomposition for inviscid transonic aerodynamics. Technical report, Singapore-MIT Alliance, 2003. URL `http://dspace.mit.edu/bitstream/handle/1721.1/3694/HPCES002.pdf?sequence=2`.

[27] T. Usyk, R. Mazhari, and A. McCulloch. Effect of laminar orthotropic myofiber architecture on regional stress and strain in the canine left ventricle. *Journal of Elasticity*, 61:143–164, 2000. ISSN 0374-3535. doi:10.1023/A:1010883920374. 10.1023/A:1010883920374.

[28] T. P. Usyk, I. J. LeGrice, and A. D. McCulloch. Computational model of three-dimensional cardiac electromechanics. *Computing and Visualization in Science*, 4 (4):249–257, July 2002. doi:10.1007/s00791-002-0081-9.

[29] F. J. Vetter and A. D. McCulloch. Three-dimensional stress and strain in passive rabbit left ventricle: A model study. *Annals of Biomedical Engineering*, 28(7):781–792, Jul 2000. doi:10.1114/1.1289469.

[30] J. C. Walker, M. B. Ratcliffe, P. Zhang, A. W. Wallace, B. Fata, E. W. Hsu, D. Saloner, and J. M. Guccione. Mri-based finite-element analysis of left ventricular aneurysm. *Am J Physiol Heart Circ Physiol*, 289:692–700, March 2005. doi:10.1152/ajpheart.01226.2004.

[31] C. Wu, Y. Liang, W. Lin, H. Lee, and S. Lim. A note on equivalence of proper orthogonal decomposition methods. *Journal of Sound and Vibration*, 265:11031110, 2003. doi:10.1016/S0022-460X(03)00032-4.